Basaltoids and Carbonatite Tuffs of Ambinsky Volcano (Southwestern Primorye): Geology and Genesis

V. K. Popov[a], S. O. Maksimov[a], A. A. Vrzhosek[a], and V. M. Chubarov[b]

[a] Far East Geological Institute, Far East Division, Russian Academy of Sciences, Vladivostok, Russia
[b] Institute of Volcanology, Far East Division, Russian Academy of Sciences, Petropavlovsk-Kamchatskii, Russia
Received March 9, 2006

Abstract—Geological–petrological data were first obtained on the Early Miocene basaltoids and spinel–fassaite carbonatite tuffs of the Ambinsky volcanic structure in southwestern Primorye. The geological study of Ambinsky volcano allowed the reconstruction of stratigraphic sections across lava and pyroclastic basaltic rocks and stratified carbonatite tuffs. The chemical compositions of rocks and mineral phenocrysts from basalts and carbonatite tuffs are reported. The basaltoids are classed with undifferentiated moderately alkaline within-plate basalts. Evidence of carbonate–silicate immiscibility was found in the basaltoids and carbonatite tuffs. It was suggested that the formation of the carbonatite melt associated with simultaneous basification and abundant crystallization of spinel, fassaite, as well as oversaturation of the silicate system in Ca was caused by limestone assimilation, subsequent transformation of the melt, and liquid immiscibility. Thermal decomposition of carbonates with dissolution of released CaO in magma and accumulation of CO_2 in a closed magmatic chamber gave rise to the autoclave gas effect and, correspondingly, heavy explosive eruptions atypical of such volcanic rocks. The genesis of carbonatite tuffs of Ambinsky volcano can serve as a model example of exsolution of carbonate melt in the moderately alkaline nonagpaitic basaltic system.

Keywords: geology, volcanism, petrology, basaltoids, carbonatites, Primorye.
DOI: 10.1134/S1819714007040069

INTRODUCTION

The genesis of carbonatites and carbonatite-like rocks remains one of the most debatable petrological problems. Therefore, new finds of these rocks provide key insight into the mechanism of their formation. Of most interest are the finds of volcanic carbonatites. Recent occurrences of volcanic carbonatites were found only within the East African rift system (Oldoinyo Lengai, Fort Portal, and other volcanoes). Late Pleistocene carbonatite lavas and tuffs are known from the Rhine graben (Kaiserstuhl volcano) and South Afghan depression (Hannenshin volcano). Volcanic carbonatites have not been found in Late Cenozoic magmatic provinces of the eastern Asian margin as yet.

When studying the Cenozoic volcanic rocks in 2000, we found carbonatite tuffs in the pyrocastic sequence of the Early Neogene Ambinsky basaltic volcano. The volcanic edifice, about 20 km² in area, is located in the middle reaches of the Amba River 28 km from its emptying into Amur Bay (Fig. 1). Basaltoids that compose stratovolcano rest immediately on the Permian carbonates and volcanosedimentary rocks, and Triassic arkosic sandstones and are unconformably overlain by Late Miocene volcanosedimentary rocks of the Ust Suifun Formation and basalts of the Shufan plateau.

This work is aimed at a geological, mineralogical, and chemical study of the basaltoids and carbonatite tuffs that compose Ambinsky volcano. Based on the obtained results, the possible formation mechanism of silicate–carbonate melts and features of the volcanic carbonatites of southwestern Primorye are considered.

GEOLOGY

The Ambinsky riftogenic depression is one of the least studied structures in southwestern Primorye. The depression is an NW-trending graben-like structure about 12 km long and 5–6 km wide situated in the Amba River basin. It is overlain by Late Miocene flood basalts of the Shufan Complex. The first data on the geological structure of the Ambinsky depression were reported in the works of B.I. Vasil'ev (1958), A.A. Asipov (1960), A.A. Vrzhosek (1968), and the explanatory note to the geological map on a scale of 1 : 200 000 [1]. The stratigraphic sections were constructed across Tertiary sedimentary and volcanogenic infill of the depression. The oldest coal-bearing volcanogenic–sedimentary rocks were combined into the Uglovsky Formation (Eocene), while the overlaying basaltoids were identified as the Sandugan Formation (Early Miocene). In the 1980s, the coal-bearing volcanogenic–sedimentary deposits were traced by prospecting drilling. These works showed that the basaltoids of the Sandugan Formation alternate with and are replaced in the depression margins by coal-bearing volcanogenic rocks of the
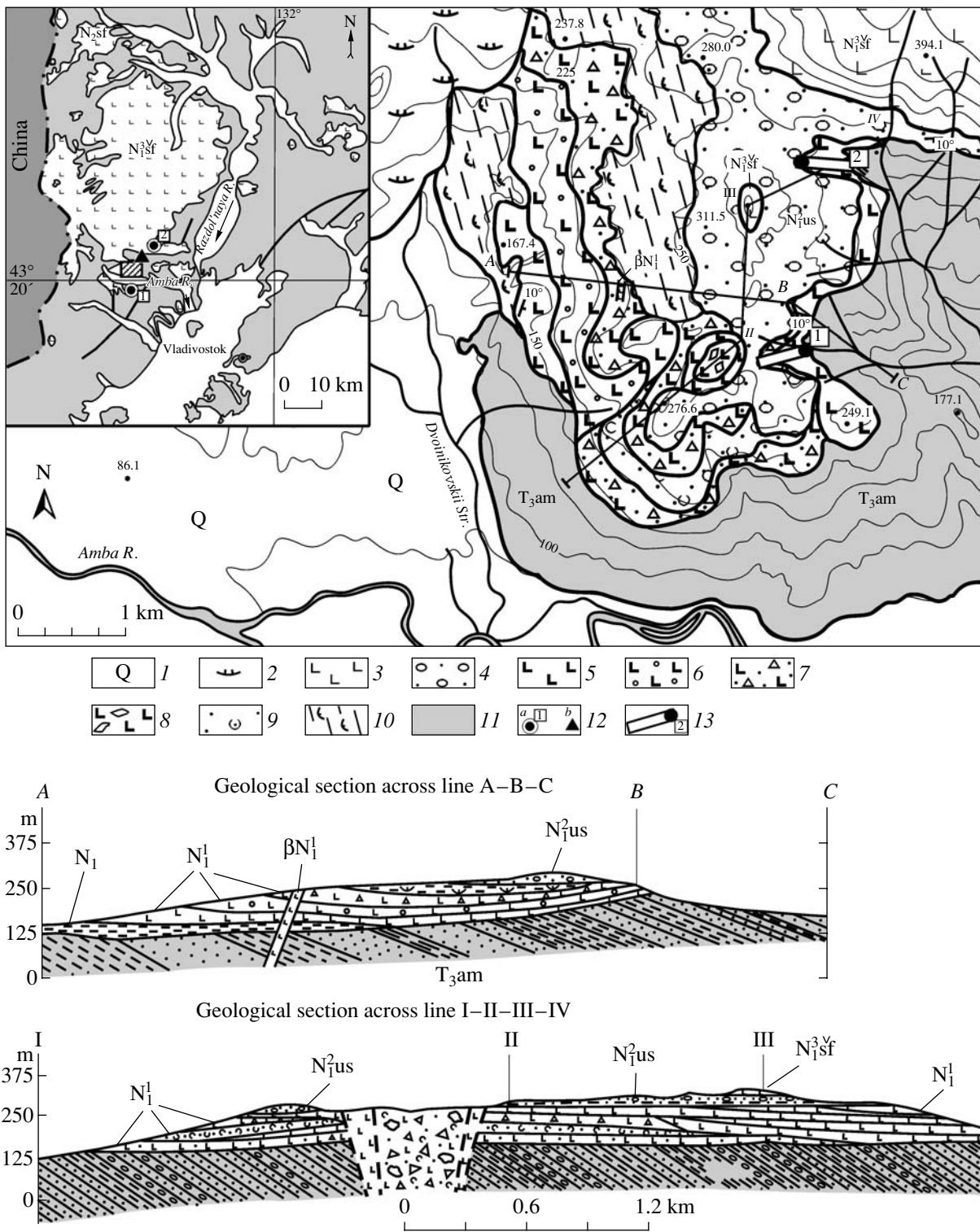
Fig. 1. Schematic geological map and sections of the central part of Ambinsky volcano. (*1*) Quaternary deposits; (*2*) landslide; (*3*) basalts of the Shufan plateau (N_1^3 š f); (*4*) sandy–gravelly deposits of the Ust-Suifun Formation (N_1^2 us); (*5–8*) rocks of Ambinsky volcano: lava flows of massive (*5*) and porous (*6*) basalts, pyroclastic cover (*7*), and vent rocks (*8*); (*9*) tuffaceous sandstones (N_1); (*1*) tuffsiltstones of coal-bearing formation (N_1); (*11*) sandstones and siltstones of the Ambinsky Formation (T_3am); (*12*) (*a*) location of a section of carbonatite tuffs in the basin of the Second stream, point P-496 (1), and peripheral edifices on the right bank of the Anan'evka River (2), (*b*) outcrops of basalts in the upper reaches of the Kedrovka River; (*13*) (1) basaltoid sequence at point P-492A shown in Fig. 2 and (2) localities of basaltoid samples downsection (sample P-492/1–P-492/5). The chemical composition of the rocks is shown in Table 4.

Uglovsky Formation (Yakushev, 1989). These authors ascribed the coal-bearing deposits to the Early Miocene Ust Davydovsky Formation. At the Fourth Regional Stratigraphic Conference in 1994, the age of the Ust–Davydovsky Formation was taken to be Late Eocene [19]. The volcanogenic–sedimentary and volcanic rocks filling the Ambinsky depression in the Amba River basin were studied in 2000 in the frameworks of GDP-200. As a result, the coal-bearing volcanogenic–sedimentary rocks and basaltoids were distinguished as the Eocene Klerkov Formation [21]. The detailed study of the volcanic rocks of the Ambinsky depression performed in 2003–2005 resulted in the revision of the age of the basaltoids and coal-bearing deposits. At present, we agree with the Late Oligocene–Early Miocene age of the considered sedimentary and volcanogenic–sedimentary rocks.

The basement rocks of the Ambinsky depression are cut by sublatitudinal (NW-trending) faults. The depression base is uplifted in the northeastern part and subsided in the southwestern part, where the most complete succession of coal-bearing volcanogenic–sedimentary rocks is observed. The sedimentary infill is gently inclined to the northeast. The coal-bearing deposits in the western part of the depression are alternated with basaltoid flows and tephra intercalations. The basaltoid volcanic edifice is confined to the southeastern side of the depression. Most its part, the central vent included, is located on the left bank of the Amba River (Fig. 1). Isolated flows of the basaltoids and tuffs that compose the peripheral parts of the volcano are exposed on the right side of the Amba River. The basaltoids penetrated by prospecting boreholes in the river valley and its right side are alternated with coal-bearing deposits (Fig. 2). The total thickness of the sequence varies from 20 to 200 meters. These deposits show lithological–facies variability. In particular, the amount of sedimentary rocks increases with the distance from the volcanic edifice, while coarse-grained sediments (conglomerates) are confined to the lowering in the depression basement topography. The sedimentary rocks are predominantly arkosic in composition, with a volcanogenic admixture. The pyroclastic material (fragments of basaltoid tephra) occasionally reaches >50%, approximating greywacke composition. The fine-grained rocks universally contain coalified plant organics and micaceous minerals, while tuffstones are abundant in spinel, pyroxene, and carbonate grains.

GEOLOGICAL STRUCTURE OF AMBINSKY VOLCANO

The Ambinsky volcanic structure represents the remains of a stratovolcano (15–20 km across at the base) whose well-preserved central vent is made up of volcanic breccia, scoria, and lavas of basalts (Fig. 1). The effusive lavas overlay sandstones and siltstones of the Ambinsky Formation. The pre-Mesozoic basement rocks are represented by Upper Permian volcanogenic–sedimentary rocks with horizons of marbleized limestones of the Barabash Formation.

The volcanic cone is composed of lavas, tuffs, and agglutinates with tuffogenic–sedimentary intercalations of variable thickness. The rocks of the volcanic edifice are cut by basaltoid lavas. The presence of pillowed basalts and hyaloclastites at the base argues that the lavas erupted in a water environment. The pyroclastic deposits of distal facies, including spinel tuffs and explosive carbonatite tuffolavas, were also formed in aqueous conditions. This is supported by the redeposition of individual tephra beds, the bedding of the rocks, the presence of plant detritus in layers, and the secondary carbonate cementation of carbonatite tuffs.

The stratigraphic section was constructed across a lava–pyroclastic sequence on the left side of the Amba River and a volcanosedimentary unit with carbonatite tuffs on the right bank of the Second Stream (the right tributary of the Amba River) 500 m upstream from the mouth (Figs. 1 and 2).

The following succession of the rocks was established on the left flank of the Amba River at the stream level (from the base upward):

(1) Massive coarse-pillow basalts with scarce zeolite-filled amygdules; the thickness is 1 m.

(2) Volcanic scoria containing intensely oxidized fragments of porous basaltoids and volcanic bombs up to 5–7 cm across, with more oxidized finer grained scoria and ash material in the groundmass. Upsection, the number and size of the fragments increase; the welding degree is high. The thickness is 4 m.

(3) Agglutinates consisting of welded rounded fragments of oxidized porous basaltoids and volcanic bombs 15–20 cm across. The rocks are cemented by small crushed fragments of oxidized basaltoids—2 m.

(4) Red-brown bedded basaltoid tephra composed mainly of small (pebble-size) fragments of volcanic scoria with less common clasts of olivine, pyroxene, plagioclase, and spinel. The rocks show a gradational structure. They are saturated in carbonate matter, and contain carbonate veinlets and pockets. The thickness is 0.4 m.

(5) Porous and amygdaloidal weakly oxidized basaltoids with platy and pillowed jointing, which laterally change into agglutinates. The thickness is 2 m.

(6) Red-brown basaltoid tephra compositionally similar to that of bed 3, with weakly expressed cross bedding. The thickness is 1.3 m.

(7) Porous and amygdaloidal basaltoids with platy and pillowed jointing, weakly oxidized, compositionally similar to bed 4. The thickness is 2.5 m.

(8) Strongly weathered, loose, oxidized basaltoids with platy joining and carbonate amygdules. The thickness is 3 m.

The total thickness is 16.2 m.

The most complete tuffogenic sequence of Ambinsky volcano with carbonatite tuffs and tuffolavas is sit-
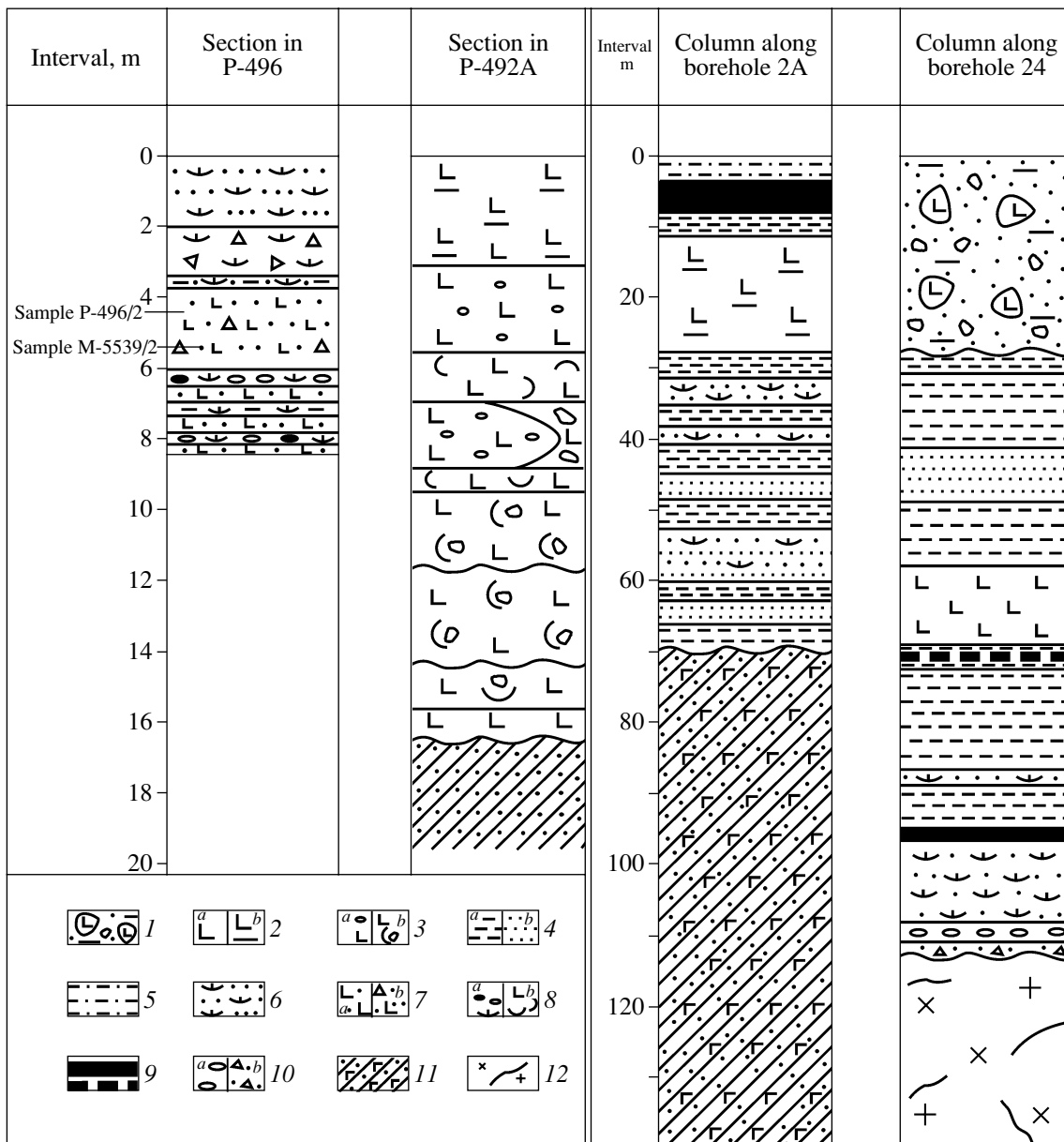
Fig. 2. Stratigraphic columns of Ambinsky volcano (P-496 and P-492) and coal-bearing volcanogenic–sedimentary rocks of the Ambinsky depression based on drilling data (boreholes 2A and 24, materials of V.V. Yakushev, 1989). (*1*) Alluvial deposits; (*2*) pillowed (*a*) and platy (*b*) basalts; (*3*) porous basaltoids (*a*), agglutinates and volcanic scoria (*b*): (*4*) siltstones (*a*) and sandstones (*b*); (*5*) silty sandstones; (*6*) tuffogenic sandstones; (*7*) lithic-crystal sand-size (*a*) and pebble-size (*b*) carbonatite tuffs; (*8*) tuffgravelstone (*a*) and tephra (*b*) of carbonatite composition; (*9*) coal seams; (*10*) conglomerates (*a*) and gruss (*b*); (*11*) Triassic sandstones of the Ambinsky Formation (*a*) and Permian volcanogenic–sedimentary rocks of the Barabash Formation (*b*); (*12*) Late Permian granodiorites of the Gamov Complex. Samples P-496/2 and M-5539/2 indicate the sampling locality of carbonatite tuffs in the section (the section is described in the text). Boreholes 2A and 24 are located on the right bank of the Amba River 6 km southwest of the peak of the main volcanic edifice with an altitude of 276.6 m (Fig. 1).

uated on the right bank of the Second Stream, 500 m upstream from the mouth. The section base unavailable for study is presumably made up of Paleozoic basement rocks, granodiorites, and spilitized basalts, which are exposed, respectively, upward and downward the stream. A basaltoid flow resting on Triassic sandstones was recovered 500 m west of the carbonatite tuff exposure in the river bed and on the banks of the Third Stream. (sample P-496/4, Table 4).

The sequence of horizontally bedded rocks is as follows (from the base upward):

(1) Dark gray pebble-size lithic-crystal tuffites with a terrigenous admixture and grains of spinel, pyroxene, and carbonates. The thickness is 0.4 m.

(2) Dark gray massive fluidal–banded tuffolavas, with alternation of thin (1–3 cm) variegated layers. The thickness is 0.3m.

(3) Dark gray homogenous sand-size tuffites with an admixture of felsic terrigenous material and thin bluish gray chalcedony lenses. More compact nodules are distinctly distinguished. The thickness is 0.06 m.

(4) Tuffs compositionally similar to those of bed 2, with silty cement and scarce lithic clasts of gray carbonatites and crystal clasts of spinel, pyroxene, and carbonates. The thickness is 0.15 m.

(5) Dark gray tuff gravelstone with lighter greenish gray pebble-size cement. The thickness is 0.03 m.

(6) Black, compact, homogenous tuffs (tufflava). The thickness is 0.3 m.

(7) Greenish gray pebble-size lithic-crystal tuffs. The thickness is 0.03 m.

(8) Dark gray to black strongly weathered (decomposed) tufflava with a clumpy central part and conchoidal top layer. The thickness is 0.3 m.

(9) Dark gray, sand-size, bedded lithic-crystal tuffs with conchodial jointing. The thickness is 0.3 m.

(10) Brown-gray tuff gravelstones with palagonitized and ferruginous cement and small pebbles of different composition. The thickness is 0.25 m.

(11) Dark gray to brownish gray ferruginous tuffo-gravelstones, with sand-size cement and conchodial jointing. The thickness is 0.10 m.

(12) Dark gray sand-to-pebble-size spinel tuffs. The lower part is made up of dense, welded tuffs with a large amount (about 5 vol %) of carbonates, spinel, pyroxene, and, more rarely, plagioclase (sample P-496/2). The central and upper parts contain coarse pillow tuffs. Long fragments of wood pipe about 5 cm across with a partially opalized core were found in the upper part. The lithic clasts (1–2 cm across) are represented by light gray and gray carbonatite and separate droplike aggregates of pink carbonate. The cement has a carbonate–silicate composition. The thickness is 2.5 m.

(13) Dark gray ochreous in the central part tuffosiltstones with numerous wood trunks and coarse plant detritus. The thickness is 2.5 m.

(14) Dark gray lithic-crystal tuffs with fragments of spinel, pyroxene, and carbonates and lithic clasts of dark gray carbonatites (1–2 cm across). The thickness is 1.3 m.

(15) Red, coarsely bedded, pebble-size tuffaceous sandstones, intensely ochreous, with spinel and carbonate clasts. The thickness is 2 m.

The total thickness of the sequence is 8.33 m.

All the facies varieties of the pyroclastic sequence are abundant in spinel, clinopyroxene, and carbonate, representing carbonatite tuffolavas and tuffs. Weathered and redeposited rocks (tuffites, tuffsiltstones, and tuffaceous gravelstones) have a similar composition and contain only an insignificant terrigenous admixture.

The maximum thickness of the Ambinsky volcanic sequence is 200 m. The wide abundance of pyroclastic rocks in addition to lavas indicates explosive eruption.

The bedrocks of basaltoids found 6 km northeast of Ambinsky volcano in the upper reaches of the Kedrovka Stream (left tributary of the Amba River) and 12 km farther in the basin of the Bol'shaya Anan'evka River (Elduga) are compositionally close to the basalts of the main edifice but insignificantly differ in petrography and geochemistry and can be considered as the peripheral volcanic edifices (daughter volcanoes) of the Ambinsky volcanic center.

PETROGRAPHY AND MINERALOGY OF THE ROCKS

The basaltoids of Ambinsky volcano strongly differ in appearance from the overlying tuffs of the Shufan plateau. These are massive rocks with large phenocrysts (0.3–0.8 cm across) of olivine, clinopyroxene, plagioclase, Ti-magnetite, and spinel of several generations accounting for from 5 to 10 vol %. Clinopyroxene contains small inclusions of olivine and spinel, as well as spinel–clinopyroxene intergrowths. The groundmass is glassy, intersertal, or doleritic (in the central part of thick lava flows). The groundmass contains plagioclase, clinopyroxene, ore minerals, and more rarely, olivine and orthopyroxene. In the individual lava flows, olivine is replaced by chlorophaeite and embedded in the chloritized groundmass. Occasionally, small amygdules are filled with chlorite in association with other secondary minerals, including zeolite and carbonate. The olivine–clinopyroxene eruptions give place to spinel–Ti-augite–plagiolcase basalts, which are mainly abundant in the daughter volcano on the Bol'shaya Anan'evka River basin. The spinel–clinopyroxene basalts contain marble xenoliths (up to 1–2 cm across) with traces of thermal decomposition. Spinel and clinopyroxene megacrysts (0.5–1.2 cm in size) occasionally contain rounded carbonate inclusions. In addition, the groundmass of the rocks contains numerous carbonate aggregates, which fill gas cavities that are widespread in the vent facies, thus, reflecting the important role of CO_2 in its evolution.

Plagioclase–hypersthene basaltic andesites occur in the Bol'shaya Anan'evka River basin, in addition to olivine and Ti-augite varieties. The rocks contain foreign quartz with a reaction clinopyroxene rim.

The composition of the rock-forming minerals is shown in Table 1. Olivine phenocrysts are higher-Mg (Fa_{26-30}) than olivine from the groundmass (Fa_{32}). The Ca and Mn contents in olivines also increase with increasing iron mole fraction (Table 1). Clinopyroxene phenocrysts have a high Al content and belong to fassaite. Clinopyroxene shows zoning with an outward decrease in the Al content and an increase in the Na content. The composition of the marginal zones is close to that of the groundmass pyroxene (Table 1, Fig. 3). Plagioclase laths are composed of high-Ca labrador (An_{64-69}). Ore minerals occur as large grains of high-Al spinel (pleonaste) and Ti-magnetite. Spinel contains an
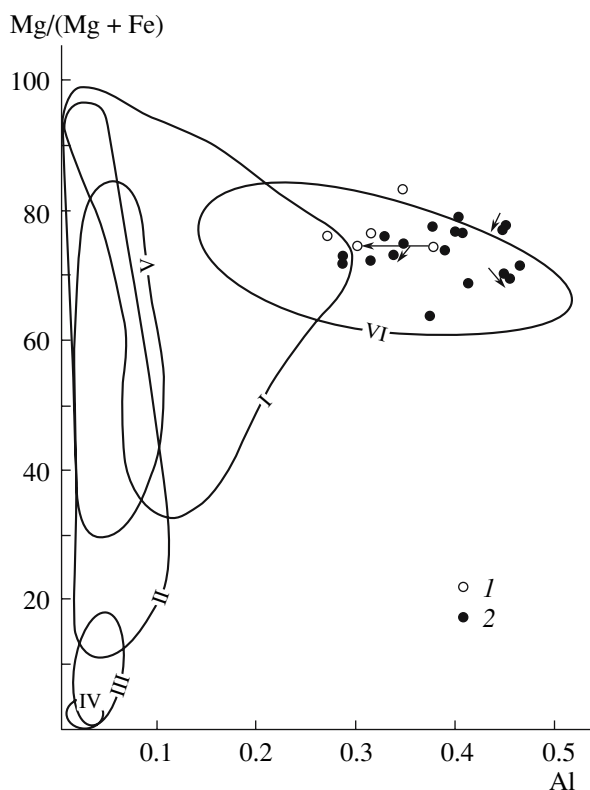
Fig. 3. Composition of pyroxenes from basaltoid lavas and carbonatite tuffs of the Ambinsky volcano in the diagram Mg/Mg + Fe (at %)–Al (f.u.). (*1, 2*) Pyroxenes from basaltoids (*1*) and carbonatite tuffs (*2*). Arrows indicate core to rim variations. Compositional fields of pyroxene: (I–IV) carbonatites of alkali ultramafic intrusions from high-temperature K-feldspar–calcite (I) and albite–calcite (II) facies to the lower temperature amphibole–dolomite–calcite (II) and chlorite–ankerite (IV) facies [20]. (V) Carbonatites of the Oldoinyo–Lengai volcano; (VI) alkali rocks of Kaiserstuhl volcano and volcanoes of the Eastern African rift system with carbonatite occurrences [6].

Photo 1. Spinel–fassaite carbonatite tuffs of Ambinsky volcano (polished samples) with silicate–carbonate (a) and carbonate (b) groundmass. Grains of spinel (black) and pyroxene in the carbonatite clasts (light) and groundmass (dark gray). Samples: (a) P-496/2; (b) M-5798.

insignificant admixture of Ti and completely lacks Cr (Table 1).

Welded carbonatite tuffs are massive, intensely welded, dark gray rocks with sand-to-pebble size crystal and lithic clasts (Photo 1). The high degree of tuff welding is related to the high content of carbonaceous matter, which caused the formation of natural carbonate–silicate cement. The tuffs contain sparse fragments of intrusive and sedimentary basement rocks. Besides the predominant welded tuffs, there are also tuffolava rocks, which are composed of compact vitrophyric carbonate–silicate aggregate with rare large phenocrysts of spinel and pyroxenes as well as gas cavities and pores that are covered by whitish films of crystalline carbonate.

The carbonatite tuffs have a crystal–lithic texture. Lithic clasts (0.2–0.5 cm in size) are white or light gray, irregular or rounded (ocellar) in shape, and account for 60–70%. They include mainly carbonate–silicate mate-

rial with phenocrysts of spinel, pyroxene, and thin laths of plagioclase (Photos 1, 2). The tuffs have high contents (up to 10 vol %) of large (up to 5–12 mm) crystals and fragments of clinopyroxene (fassaite), high-Al spinel (pleonaste), and less common hercynite and high-Al Ti-magnetite (Tables 2, 3). Pyroxenes from carbonatite tuffs and basalts have a high content of Al up to 11 wt % (0.30–0.45 f.u. Al) and Ti (up to 8.95 wt % TiO_2) at a lowered content of SiO_2 and, according to the accepted classification [14], can be classed (except for sample M-5539/2, Table 3) with typical fassaite. The oxidation state of iron in pyroxenes calculated from the ferrous to ferric ratio in tschermakite end member varies within 0.38–0.66. Pyroxene crystals have weakly expressed zoning showing an outward decrease in the Mg number and an increase in the iron mole fraction at an insignificant content of Na (Table 3, Fig. 3). As compared to pyroxenes from typical carbonatite complexes around the world, the pyroxenes from the studied carbonatite tuffs are higher in Ti, Al, and Mg and show no enrichment in the aegirine end member. At the same time, the Al_2O_3 content in them is close to that in pyroxenes from alkali mafic volcanic complexes associated with carbonatites (Fig. 3). Similar high-Al pyroxenes are known from vent basalts in the Neogene volcanic edifices of Primorye [3]. However, pyroxenes

Table 1. Composition of minerals from basaltoids of Ambinsky Volcano

Mineral	Olivine				Clinopyroxene			Spinel	Ti-mag-netite	Plagioclase	
Ordinal No.	1	2	3	4	5	6	7	8	9	10	11
SiO_2	38.25	37.54	37.01	37.40	45.28	48.17	46.55			50.06	50.72
TiO_2	0.00	0.05	0.03	0.09	3.74	2.05	3.45	0.71	24.47	0.14	0.20
Al_2O_3					8.49	6.82	6.06	56.68	2.53	31.69	30.90
Cr_2O_3								0.22		0.06	
FeO*	23.53	26.93	27.86	27.11	7.28	7.64	6.97	29.73	62.99	0.40	0.61
MnO	0.30	0.45	0.50	0.53	0.03	0.07		0.15	0.51		
MgO	37.01	33.56	33.48	33.04	11.61	12.29	11.96	12.39	3.57	0.02	0.01
CaO	0.10	0.32	0.42	0.35	22.39	21.73	22.44		0.26	14.35	13.87
Na_2O	0.01				0.30	0.52	0.51			3.42	4.10
K_2O	0.04	0.03	0.05	0.03	0.03	0.03	0.03	0.06	0.03	0.12	0.14
Cy	99.24	98.88	99.35	98.55	99.15	99.32	97.97	99.72	94.58	100.26	100.55
f	26.3	31.1	31.4	31.5	26.0	25.8	24.6	50.5	80.0		
Fo	73.7	68.6	68.2	68.5							
Wo					50.6	48.5	50.4				
En					36.5	38.2	37.4				
Fs					12.9	13.3	12.2				
An										69.4	64.6

Note: sample P-490/1. Phenocrysts: (1, 2, 5, 7) core; (6) rim; Groundmass: 4, 3, 10, 11; (8–9) inclusions in clinopyroxene (an. 5).
* All iron was determined as FeO. Hereinafter, a dash denotes that an element was not detected. $f = 100 \times FeO/FeO + MgO$ (at. %). Hereinafter, the minerals were analyzed using a Camebax microprobe at the Institute of Volcanology and Seismology, Far East Division, Russian Academy of Sciences; accelerating voltage of 20 kV and ion current of 40 nA. Synthetic and natural standards of known compositions were used for comparison. Analyst—V.M. Chubarov.

from the carbonatite tuffs have a higher Al_2O_3 content. Spinels in the rocks under consideration are close to pleonastes from the basaltoid lavas and also contain an insignificant amount of TiO_2 (up to 1.65 wt %). The iron mole fraction in Al-spinels widely varies ($f = 35–51$), though individual grains show insignificant core-to-rim changes (Fig. 3). Pyroxenes from the carbonatite tuffs contain droplike inclusions of aluminous Ti-magnetite and Al–Cr spinels, which are close in composition to high-Al chromites from lherzolite inclusions in alkali basalts of Primorye [22]. The distinct mineralogical feature of carbonatite tuffs is their universal enrichment in relatively large (up to 0.5 cm) euhedral crystals of orange, transparent white (more rarely), or cherry red flatten rhombohedral Fe–Mg calcite. This mineral, similar to other minerals, is distributed over the carbonate–silicate groundmass and carbonate ocelli embedded in the latter. Calcites often grow together with spinel and pyroxene and contain microinclusions of these minerals (photo 2). In turn, the clinopyroxene and spinel host two-phase carbonate melt inclusions, as well as drop-like macroinclusions of carbonate melt. Spinels and clinopyroxenes from the carbonatite volcaniclastic rocks are characterized by significant variations (Tables 2, 3).

Tuffolavas are enriched in white and (more rarely) lilac oval silicate–carbonate segregations (ocelli), which are 10–12 mm in size, have sharp contacts with the groundmass, and contain evenly distributed liqua-tion drops of the carbonate melt (Photo 2). The carbonatite occelli show distinctly expressed fluidity due to parallel alignment of flattened carbonate drops and bytownite laths. The carbonate drops occasionally contain microdrops of iron sulfides or are rimmed by them (photo 2). The carbonate globules have an orange color and correspond to Fe–Mg calcite (Table 2).

CHEMICAL AND TRACE ELEMENT COMPOSITION

Basaltoids have low SiO_2 content and relatively high contents of TiO_2, MgO, CaO, and Na_2O (Table 4). In the classification diagrams, the data points are plotted in the fields of basanites and basalts (Fig. 4). In terms of the HFSE abundance, they correspond to within-plate alkali basalts (Fig. 5). They contain 0.1–13% CIPW-normative nepheline and 12–25% albite. The basaltoids from the daughter volcano differ in lower MgO content and higher contents of alkalis, LILE (Rb, Ba, Sr), HFSE (Zr, Th), and REE. Trachybasaltic andesites show a decrease in Al_2O_3, MgO, and CaO and an increase in the K_2O content (Table 4). As compared to typical carbonatites, the carbonatite tuffs are higher in SiO_2, Al_2O_3, and TiO_2 at wide variations of CaO (Table 4). The HFSE content in these rocks is close to those in the basaltoids of Ambinsky volcano. In addition, they are characterized by high contents of compat-
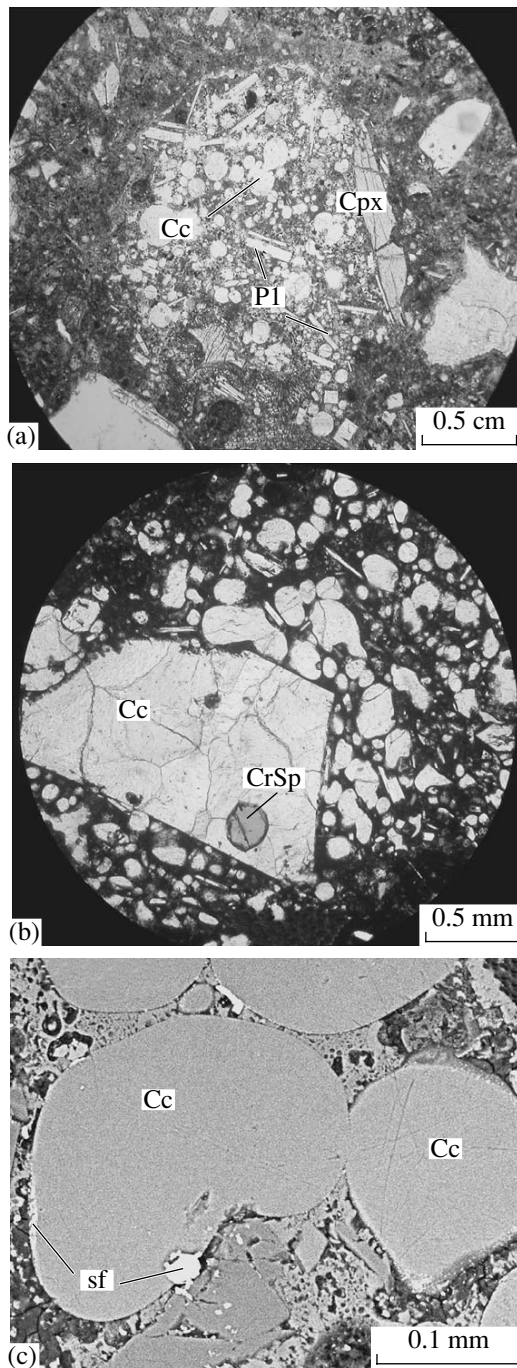
Photo 2. Thin sections: (a) carbonatite ocelli with calcite globules (Cc) containing crystals of plagioclase (Pl) and fassaite (Cpx); (b) crystals of Fe–Mg calcite (Cc) with inclusions of Cr-spinel (CrSp) in the carbonatite ocelli consisting of Fe calcite globules in a silicate–carbonate groundmass; (c) globules of Fe–Mg calcite (Cc), light are sulfides (sf); Sample M-5539/2.

Fig. 4. Diagram ($Na_2O + K_2O$)–SiO_2 [31] for basaltoids of the Ambinsky volcano. Numbers denote fields: (1) basanites (Ol > 10%) and tephrites (Ol < 10%); (2) phonotephrites; (3) tephrophonolites; (4) trahybasalts; (5) basaltic trachyandesites; (6) trachyandesites; (7) picrobasalts; (8) basaltic andesites.
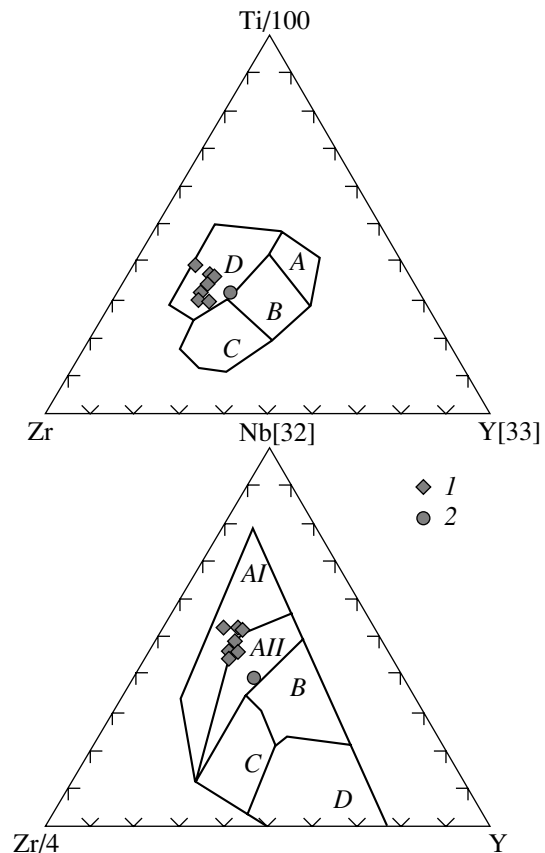
Fig. 5. Diagram Zr–Ti–Y [33] and Zr–Nb–Y [32] for basaltoids (1) and carbonatite tuffs (2) of Ambinsky volcano. Fields in the diagram Zr–Ti–Y: (A) island arc tholeiites, (B) mid-ocean ridge basalts (MORB), island-arc tholeiites and calc-alkaline basalts; (C) calc-alkaline basalts; (D) within-plate basalts. Fields in the diagram Zr–Nb–Y: (AI) within-plate alkali basalts; (AII) within-plate alkali basalts and within-plate tholeiites; (B) E-type MORB; (C) within-plate tholeiites and island arc basalts; (D) N-type MORB and island arc basalts.

ible elements (Ni, Cr, V), LILE (Sr, Ba, and Cs), and HFSE (Zr). The primitive mantle-normalized trace element distribution for the basalts shows positive Ba, Nb, La, Sr anomalies and negative Hf anomaly. The carbon-

Table 2. Composition of minerals from carbonatite tuffs of Ambinsky volcano

Upper strip — Plagioclase and Spinel

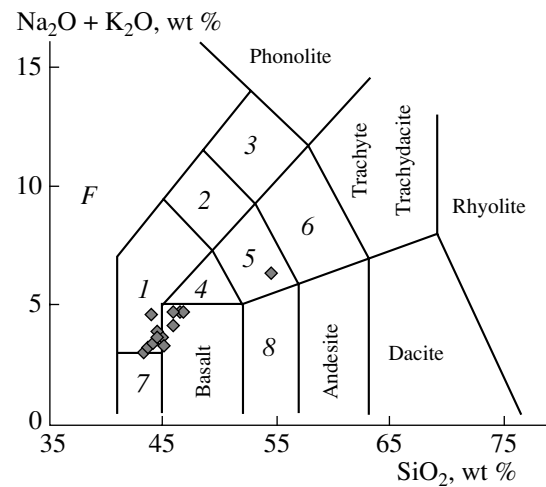| Measurement point	Plag M-5534	Plag M-5534	Plag M-5539/2	Plag M-5539/2	Sp P-469/2 Core	Sp P-469/2 Rim	Sp P-469/2 Core	Sp P-469/2 Rim	Sp M-5539/2 Core	Sp M-5539/2 Rim	Sp M-5539/2	Sp M-5539/2	Sp M-5539/2	Sp M-5539/2 Incl.
SiO$_2$	49.08	48.03	55.43	50.49										
TiO$_2$	0.06	0.00			1.62	1.43	0.65	0.64	1.38	1.42	0.56	0.73	16.12	0.43
Al$_2$O$_3$	31.07	32.63	27.74	30.63	56.78	57.62	61.12	61.49	56.90	55.85	62.41	58.83	14.87	54.23
Cr$_2$O$_3$												0.02	0.00	8.85
FeO*	0.53	0.39	0.40	0.78	27.25	26.17	19.31	19.24	26.76	25.17	18.69	24.91	60.43	18.41
MnO					0.05	0.07	0.04	0.01	0.06	0.07	0.05	0.06	0.24	0.06
MgO	0.21	0.07			15.01	15.33	17.38	17.92	14.36	14.47	19.02	16.23	6.98	18.25
CaO	14.92	16.00	10.43	14.47				0.04	0.04	0.03	0.20			
Na$_2$O	3.34	3.05	4.91	3.10	0.02	0.01	0.04	0.04	0.05	0.05				
K$_2$O	0.22		0.74		0.01	0.09		0.01		0.02				
NiO							0.10	0.04						
ZnO							0.02	0.04		0.01				
Cy	99.43	100.17	99.65	99.47	100.74	100.72	98.66	99.47	99.55	97.09	100.93	100.78	98.64	100.23
An	70	74	54	73										

Lower strip — Spinel, Ti-magnetite, Carbonate

Measurement point	Sp M-5539/2 Incl.	Sp M-5539/2 Incl.	Sp M-5539/2 Incl.	Ti-mag M-5534 Core	Ti-mag M-5534 Rim	Carb M-5534	Carb M-5534	Carb M-5534	Carb M-5534 Glob.	Carb M-5534 Glob.
SiO$_2$										
TiO$_2$	0.56	1.26	0.73	14.13	20.41					
Al$_2$O$_3$	62.41	57.66	46.85	14.22	5.79					
Cr$_2$O$_3$	0.05	0.07	15.32		0.19					
FeO*	18.69	26.72	20.32	59.17	63.20	2.20	5.22	1.40	2.31	2.06
MnO			0.15	0.33	0.40	2.30	1.09	1.00	1.07	0.75
MgO	19.02	15.61	16.54	7.68	6.60	2.23	2.50	1.80	2.09	2.05
CaO	0.02		0.01	0.67	0.57	55.82	47.24	52.90	47.98	47.22
Cy	100.75	101.32	99.92	96.20	97.16					

Note: the minerals in sample M-5534 were determined using a JXA-5A microprobe at an accelerating voltage of 20 kV at the Institute of Volcanology and Seismology, Far East Division, Russian Academy of Sciences (analyst—N.A. Ekimova). Synthetic and natural standards of known composition were used for comparison. (Incl.) inclusion in clinopyroxene (sample M-5534). Glob. is carbonate globules from ocellus.

Table 3. Composition of clinopyroxenes from carbonatite tuffs of Ambinsky volcano

	Sample P-469/2						Sample M-5534			Sample M-5539/2			
	Core	Rim	Core	Rim	Core	Rim			Core				
SiO_2	46.67	46.99	45.97	46.78	46.71	48.46	46.79	44.70	48.24	45.56	47.11	45.67	47.99
TiO_2	2.20	2.28	2.97	3.00	2.80	0.90	2.32	2.05	0.70	8.95	2.21	3.19	0.77
Al_2O_3	10.38	10.25	10.26	10.33	7.81	7.59	10.80	9.14	7.86	6.60	8.94	6.37	9.25
Cr_2O_3							0.30		0.61		0.06		
FeO^*	6.82	6.82	8.84	8.72	7.40	8.37	8.64	7.91	5.73	12.13	8.90	8.54	7.44
MnO			0.10		0.03	0.08	0.28	0.10	0.20	0.04	0.03	0.04	0.10
MgO	12.74	12.62	11.46	10.88	12.01	12.40	11.81	13.81	15.53	16.97	13.72	12.63	15.00
CaO	20.64	20.62	18.99	18.50	21.86	19.78	19.71	20.35	19.10	9.60	18.37	21.74	18.22
Na_2O	1.15	1.11	1.44	1.21	0.60	1.02	1.15	0.94	0.53	0.06	1.23	0.51	0.75
K_2O	0.01			0.03		0.01	0.01	0.02					
Cy	100.61	100.69	100.03	99.45	99.22	98.61	101.81	99.02	98.50	99.97	100.57	98.69	99.52
Si	1.719	1.727	1.715	1.745	1.757	1.824	1.715	1.690	1.798	1.687	1.743	1.743	1.774
Al^{IV}	0.281	0.273	0.285	0.255	0.243	0.176	0.285	0.310	0.202	0.278	0.257	0.257	0.226
Ti^{IV}										0.035			
Al^{VI}	0.169	0.171	0.166	0.199	0.103	0.161	0.182	0.097	0.143		0.132	0.030	0.176
Ti	0.061	0.063	0.083	0.084	0.079	0.025	0.064	0.059	0.020	0.214	0.062	0.092	0.022
Cr							0.009		0.018		0.002		
Fe	0.210	0.210	0.276	0.272	0.233	0.263	0.264	0.250	0.179	0.376	0.276	0.273	0.231
Mn			0.003	0.002	0.001	0.002	0.009	0.003	0.007	0.002	0.001	0.002	0.003
Mg	0.699	0.691	0.637	0.605	0.673	0.695	0.645	0.779	0.862	0.937	0.756	0.718	0.826
Ca	0.814	0.812	0.759	0.739	0.881	0.798	0.772	0.825	0.764	0.381	0.729	0.890	0.721
Na	0.082	0.079	0.104	0.087	0.043	0.074	0.081	0.068	0.038	0.004	0.089	0.037	0.053
K				0.001				0.002					
Cy	4.035	4.026	4.028	3.989	4.013	4.018	4.026	4.083	4.031	3.914	4.047	4.042	4.032
f	23.1	23.3	30.3	31.0	25.7	27.5	29.0	24.3	17.2	28.6	26.7	27.5	22.7
Wo	47.2	47.4	45.4	45.8	49.3	45.4	46.0	44.5	42.3	22.5	41.4	47.3	40.6
En	40.6	40.4	38.1	37.4	37.7	39.6	38.3	42.0	47.8	55.3	42.9	38.2	46.5
Fs	12.2	12.2	16.5	16.8	13.0	15.0	15.7	13.5	9.9	22.2	15.7	14.5	12.9

Table 4. Major- (wt %) and trace-element (ppm) composition of basalts and carbonatite tuffs from Ambinsky volcano

Sample No.	P-490/1	P-491/1	P-492/1	P-492/3	P-496/4	P-492/5	G-425/b	As-1	M-5407/1
Ordinal No.	1	2	3	4	5	6	7	8	9
SiO_2	44.56	44.18	43.89	43.39	43.94	44.77	45.52	45.78	46.63
TiO_2	2.20	2.31	2.41	2.27	1.97	2.17	2.56	2.07	2.25
Al_2O_3	15.81	15.37	17.00	15.34	14.70	15.79	16.96	15.20	17.89
Fe_2O_3	2.50	8.59	9.65	6.70	5.51	3.48	5.16	2.52	4.69
FeO	7.40	2.52	1.31	3.71	4.55	6.30	3.96	7.69	5.08
MnO	0.18	0.19	0.12	0.18	0.14	0.16		0.02	0.16
MgO	9.00	6.43	3.06	9.36	7.34	9.91	7.09	9.82	5.61
CaO	9.50	9.57	10.62	9.74	10.15	9.76	10.07	10.06	8.34
Na_2O	3.03	2.85	2.45	2.36	3.28	2.62	2.90	2.20	3.36
K_2O	0.68	0.66	0.91	0.69	1.26	1.05	0.95	0.72	1.43
P_2O_5	0.42	0.40	0.46	0.41	0.39	0.39	0.39	0.78	0.44
CO_2									
H_2O	0.51	1.99	1.91	0.85	1.39	0.34			0.70
L.O.I.	3.83	4.51	5.72	4.57	4.88	3.11	4.30	3.01	3.12
Total	99.62	99.57	99.51	99.57	99.50	99.85	100.26	99.87	99.70
Ni	160	160	110	120	120	167			65
Co	46	44	39	36	28	49			23
Cr	210	190	48	170	170	217			66
V	140	150	170	150	120	236			130
Rb	15	23	84	15	12	27			58
Cs									18.4
Sr	766	724	918	821	782	1085			1303
Ba	706	657	518	781	771	528			1084
Y	16	23	29	29	24	25			34
Zr	158	168	222	165	194	180			225
Nb	31	31	34	36	32	39			38
Ta	6	5	6	6	6	2			2.7
Hf			7.0	7.0	7.0	4.1			5.6
La						25			68
Ce						53			118
Pr						6.7			16
Nd						25			70
Sm						4.9			12
Eu						1.92			3.4
Gd						5.2			10
Tb						0.7			1.3
Dy						4.4			6.8
Ho						0.9			1.3
Er						2.1			3.65
Tm						0.33			0.48
Yb						1.80			2.47
Lu						0.26			0.41
Pb						2.2			4.2
Th						2.83			5.52
U						0.80			0.85
Th/U						3.5			6.5
K/Nb	91.0	88.3	111.0	75.5	163.0	111.7			156.1
Ce/Pb						25.0			28.1

Table 4. (Contd.)

Sample No.	M-5704/2	M-5426	M-5428	M-5517	M-5430	M-5539/2	P-496/2	M-5537
Ordinal No.	10	11	12	13	14	15	16	17
SiO_2	46.69	45.78	46.22	45.16	54.68	30.93	33.36	23.31
TiO_2	2.41	2.28	2.31	2.34	2.21	1.13	1.30	1.88
Al_2O_3	17.86	16.99	17.44	17.30	14.27	12.62	11.53	11.70
Fe_2O_3	5.69	5.41	5.15	8.05	3.15	3.04	4.17	2.64
FeO	4.67	5.49	4.97	2.68	4.97	2.34	1.85	1.52
MnO	0.19	0.13	0.13	0.42	0.24	0.46	0.17	0.33
MgO	4.60	6.09	5.69	5.39	3.65	4.60	6.81	2.76
CaO	9.07	9.26	8.53	11.21	5.91	22.72	16.29	27.72
Na_2O	2.46	3.44	3.67	2.40	2.92	0.90	1.03	0.88
K_2O	2.16	1.16	0.88	0.88	3.32	0.56	0.64	0.15
P_2O_5	0.61	0.59	0.56	0.56	0.85	0.23	0.25	
CO_2						13.95	14.07	20.93
H_2O	0.74	0.30	0.68	1.94	0.58	1.79	2.60	1.03
L.O.I.	2.47	2.78	3.38	4.20	2.81	4.91	6.46	4.78
Total	99.62	99.70	99.61	99.53	99.56	100.18	100.53	99.63
Ni	65		130				100	
Co	23		33				28	
Cr	66		115				69	
V	130		140				110	
Rb						23		
Cs						5.31		
Sr						518		
Ba						527		
Y						18		
Zr						90		
Nb						13		
Ta						5.31		
Hf						2.7		
La						19		
Ce						30		
Pr						39*		
Nd						18		
Sm						3.3		
Eu						1.13		
Gd						3.7		
Tb						0.56		
Dy						3.23		
Ho						0.60		
Er						2.12		
Tm						0.26		
Yb						1.42		
Lu						0.21		
Pb						4.5		
Th						2.18		
U						0.69		
Th/U						3.1		
K/Nb						178.8		
Ce/Pb						6.6		

Note: (1–8) Ambinsky volcano; (9–13) peripheral volcanic edifice in the Bol'shaya Anan'evka River Basin; (15–16) carbonatite tuffs and (17) carbonatite ocelli from carbonatite tuffs of the Ambinsky edifice. The anomalous contents of Pr in sample M-5539/2 (noted by asterisks) is erroneous and replaced by the value of 3.97 obtained by interpolation relative to the chondrite-normalized Ce and Nd contents. The silicate analyses were performed by wet chemistry at the analytical center of the Far East Geological Institute, Far East Division, Russian Academy of Sciences, (analyst—L.I. Alekseev); the trace elements in samples P-492/5, M-5407/1, and M-5539/2 were analyzed by ICP-MS at the Vinogradov Institute of Geochemistry and Analytical Chemistry, Siberian Division, Russian Academy of Sciences (analyst—G.P. Sandimirova); other data were obtained by optical spectroscopy (Ni, Co, Cr, V) and XRF analysis (analysts—L.I. Azarova and E.A. Nozdrachev) at the Far East Geological Institute. Sample G-425-b is taken from A.A. Vrzhosek (1968). Data As-1 are from A.A. Asipov (196). Dashes denote that an element was not found; a gap denotes that the data are absent.
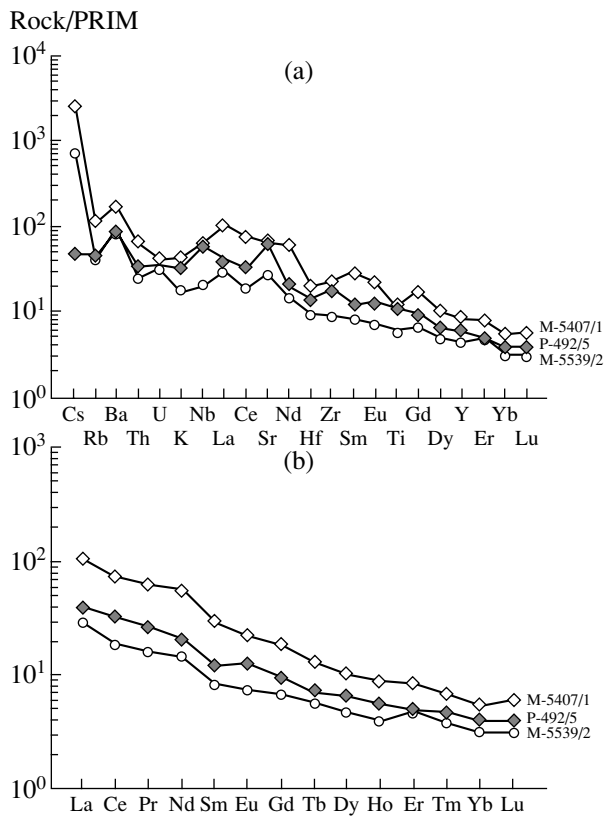
Rock/PRIM

(a)

(b)

Fig. 6. Primitive mantle normalized [34] distribution patterns for incompatible (a) and rare earth (b) elements in the basaltoids and carbonatite tuffs of Ambinsky volcanoThe trace element abundance is shown in Table 4. M-5407/1 and P-492/5 are basaltoids; M-5539/2 is carbonatite tuff.
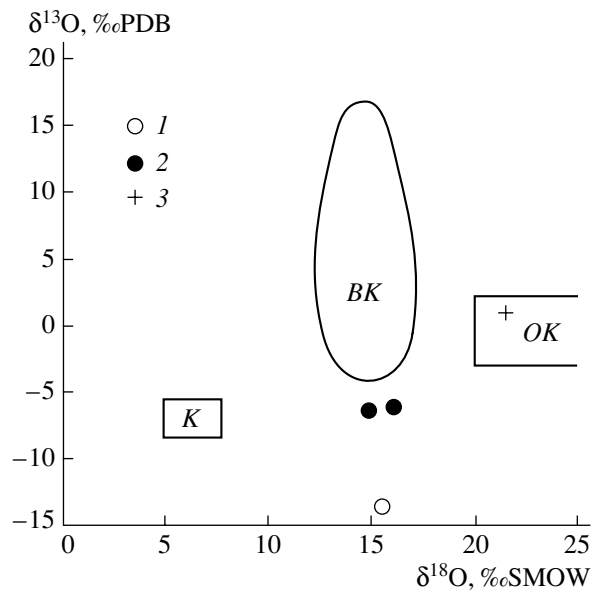

Fig. 7. Oxygen and carbon isotope composition of carbonates from basaltoids (*1*) and carbonatite tuffs (*2*) of Ambinsky volcano and marbled limestones of the Barabash Formation (*3*). Lines bordering the fields: (*K*) typical magmatic carbonatites; (*BK*) carbonatites of alkali basalts and ultramafic volcanic rocks of Kamchatka; (*SC*) sedimentary carbonatites, according to [16].

atite tuffs also exhibit positive anomalies of Cs, Ba, La, and Sr and negative anomalies of Th, K, and Ce. The basaltoids and carbonatite tuffs have moderately fractionated right-dipping trace-element distribution patterns (Fig. 6). The basaltoids and related carbonatites are characterized by a high Cs content, which was also noted for the Dayan alkali-picrite complex in the Amur region [10] and the picrite–meimechite complex of Primorye [8]. This is possibly related to the evolution of alkali basaltic magmas under the effect of alkali-hydrocarbonic fluids.

The carbon and oxygen isotope compositions in calcites from basalts (sample P-492/9: $\delta^{13}C_{PDB}$ = −13.5, $\delta^{18}O_{SMOW}$ = 15.7) and carbonatite tuffs (sample M-5533: $\delta^{13}C_{PDB}$ = −5.9; $\delta^{18}O_{SMOW}$ = 16.2; sample M-5534: $\delta^{13}C_{PDB}$ = −6.0; $\delta^{18}O_{SMOW}$ = 14.9) significantly differ from those in calcites from the basement Permian limestones ($\delta^{13}C_{PDB}$ = + 2.0, $\delta^{18}O_{SMOW}$ = +23.2, data from [7]) and, in terms of $\delta^{13}C$ values, correspond to carbonatites. The oxygen and carbon isotope composition of carbonatite tuffs is close to those of alkali and ultramafic rocks from Kamchatka, while carbonates from the basaltoids are characterized by lower values of $\delta^{13}C$ (Fig. 7).

DISCUSSION

The obtained geological and petrological data on the volcanic rocks of the Ambinsky edifice give insight in genesis of basalts and carbonatite tuffs that are related to the explosive phases of volcanic activity.

The basaltoid volcanism of the Ambinsky depression that occurred 24 ± 3 Ma ago (Table 5) significantly differs in composition and evolution from the simultaneous Oligocene–Early Miocene volcanism of the Sineutesovsky and Poimensky (Slavyansky) rift depressions in southwestern Primorye. Basalts, andesites, and dacites erupted in the Poimensky depression in the Early Miocene and were distinguished as the Slavyansky complex [21]. Dacites that complete the basic-to-acid evolution of this volcanic complex yielded an Rb–Sr isochron age of 22.9 ± 0.3 Ma [18]. Trachybasalts with a K–Ar age of 22.0 ± 1.0 Ma erupted in the Sineutesovsky depression located 30 km southwest of Ambinsky volcano [17]. The high-Al potassic basalts of the Slavyansky complex have distinctly expressed geochemical subduction signatures, while the younger andesites and dacites bear a crustal imprint [18]. The geochemistry of the trachybasalts from the Sineutesovsky depression also indicates the interaction of basaltic melts with felsic crustal material [17].

Petrogeochemically, the basaltoids of Ambinsky volcano are close to Early Miocene within-plate subalkaline basalts from the adjacent areas of East China [23, 27].

The evolution of Ambinsky volcano that produced carbonate–silicate melts with subsequent liquid immis-

Table 5. Results of K–Ar age determinations for basalts of the Ambinsky edifice

Sample No.	Rock	Locality	Potassium, % ±σ	$^{40}Ar_{rad}$ (ng/g) ±σ	Age, Ma ±2σ
–1974/1	Basaltoid	Kedrovka stream, left tributary of the Amba River	0.81 ± 0.015	1.35 ± 0.08	24 ± 3

Note: determinations were made at the Laboratory of Isotope Geochemistry and Geochronology of the Institute of Geology of Ore Deposits, Petrography, Mineralogy, and Geochemistry, Russian Academy of Sciences. Radiogenic Ar was analyzed using an MI-1201 IG mass spectrometer by isotope dilution using tracer ^{38}Ar; K was determined by flame photometry. The following constants were used in the calculations: $\lambda_K = 0.581 \times 10^{-10}$ yr^{-1}; $\lambda_{\beta-} = 4.962 \times 10^{-10}$ yr^{-1}; ^{40}K = 0.01167 (at. %). Analyst—V.A. Lebedev. Unpublished results were kindly given by Corresponding Member of the RAS V.G. Sakhno.

cibility was also evidently determined by crustal assimilation in the given case of carbonate material represented by marbled limestones of the Barabash Formation. It should be noted that the limestone bed that underlies the volcano and is exposed 8 km west of it has a thickness of 400 m. The appearance of trachybasaltic andesites with foreign quartz in the Ambinsky volcanic edifice indicates that basaltic magma assimilated felsic material in the intermediate chamber.

According to [18], the mantle and crustal components of the Cenozoic volcanic rocks of Primorye are well distinguished by their Ce/Pb and K/Nb ratios, which do not change during the crystallization differentiation of the basaltic magma and reflect the composition of the melting protolith [35]. The basaltoids of Ambinsky volcano are similar to the oceanic basalts in their Ce/Pb (25.0–28.1) and K/Nb (75.5–156.1) ratios [35] but differ in their higher Nb content relative to K. The carbonatites have a lower Ce/Pb ratio (up to 6.6) and higher (up to 178.8) K/Nb ratio. The Th/U ratio in the basaltoids and carbonatites varies from 3.2 to 6.5 and also corresponds to that in the oceanic basalts. The basaltic volcanism of the Ambinsky depression was evidently related to the repeated emplacement of sublithospheric melts and records the initial stage of Late Cenozoic volcanism that occurred simultaneously with the opening of the Sea of Japan in the Oligocene–Miocene [18]. Thus, our data indicate that the basaltoids of the Ambinsky volcano were derived from a deep-seated source without a significant contribution of felsic crustal material. However, a decrease of the Ce/Pb values at practically constant K/Nb and Th/U ratios in carbonatites marks the involvement of limestones in the melting (Table 4).

The phenocryst assemblage (olivine, fassaite, and pleonaste) in the basaltoids and unusually high content of Al-rich phases (fassaite and Al-spinel) in the carbonatite tuffs coupled with the low Ti content in spinels indicate that basaltic melts were basified during assimilation of carbonate matter. This led to the formation of high temperature silicate carbonate magma, which was immiscibly split under high CO_2 pressure [11, 12]. The thermal decomposition of carbonates with dissolution of CaO in basaltic magma and accumulation of CO_2 in a closed magmatic chamber could lead to recurrent appearance of the autoclave gas effect and powerful explosive eruptions.

The presence of high-Al magmatic clinopyroxenes in the volcanic rocks is typically interpreted as indicating high P–T crystallization conditions, which is consistent with experimental data [24] and typically used to estimate the magma generation depth and crystallization conditions for different volcanic series [5]. At the same time, the formation of high-Al fassaite clinopyroxenes in association with spinel (the typical skarn assemblage) can be defined by chemical factors and was related with assimilation of carbonate material by aluminosilciate magma with subsequent basification and depolymerization of the magmatic melt [4]. This is caused by a coordination change of Al (from ^{IV}Al to ^{VI}Al) in the aluminosilciate liquids, which shifts the system towards the fassaite and spinel stability field at low P–T conditions. A sharp widening the stability field of aluminous phases (fassaite, spinel) is related to the basification of the melt, its saturation with carbonate ion CO_3^{2-}, and limitation of the Al and Cr solubility [2]. The ilmenite–magnetite–plagioclase–olivine assemblage of the basaltic field is replaced by a spinel–fassaite–Ti-magnetite–calcite one.

The high-Al minerals (fassaite) also could crystallize during interaction of aluminosilciate melt with deep-seated alkali–carbonate fluid, which, for example, defined the specific regime during formation of the carbonatite-bearing urtite–ijolite complexes of Tuva and Kuznetsk Alatau [9].

The formation of carbonate drops in basaltic magmas owing to carbonate–silicate liquid immiscibility could result from high affinity of hydrocarbonic acid to Ca, which leads to its extraction from silicate melts by flow of gas bubble, i.e., during their barbotage by CO_2 fluid, as in the model in [15, 26]. Immiscibility also can be caused by assimilation of carbonate material and recycling of carbonates via magmatic melt with a change of its isotope–geochemical characteristics. In particular, the carbon isotope composition of calcites ($\delta^{13}C_{PDB}$ = + 2.0) from the Barabash Formation developed in the Ambinsky volcano basement corresponds to the composition of sedimentary carbonates, while those from the carbonatite tuffs correspond to typical carbon-

atites ($\delta^{13}C_{PDB}$ = –5.9 and –6.0). The calcite from the basalts has a low $\delta^{13}C$ (–13.5) but is similar to carbonatite tuffs in its $\delta^{18}O$ value (Fig. 7).

The maximum accumulation of Ca and CO_2 fluid in a silicate system leads to the instability of the system, immiscible splitting, and exsolution of carbonate liquid [13]. In our opinion, microdrop carbonate globules in silicate melts, similar to [25, 28, 30], support the existence of two equilibrium unmixed liquids.

As compared to typical carbonatites, the carbonatite tuffs and liquation ocelli are enriched in the silicate component and have the lowered contents of REE, Nb, and Zr even relative to basalts of Ambinsky volcano (Table 4). This is consistent with the preferential REE distribution in a silicate melt relative to a carbonate one [13] during carbonate–silicate liquid immiscibility in essentially calcareous low-alkali systems. The carbonatite tuffs of the Ambinsky volcanic edifice could serve as a model example of this process.

CONCLUSIONS

The occurrence of volcanic carbonatite tuffs related to moderately alkali basalts was found in the Ambinsky volcano, southwestern Primorye.

Geological and petrological data indicate that the bedded volcanoclastic unit of carbonatite tuffs and tuffolavas was formed by repeated volcanic explosions with formation of gas-saturated pyrocalstic flows, which were deposited in the lowered, often water-flood areas.

The rocks of the Ambinsky volcanic structure correspond to undifferentiated moderately alkali within-plate basalts with signs of assimilation of crustal carbonate (Ambinsky volcano) and felsic (the peripheral volcanic edifice) materials.

The formation of carbonatite melt was caused by a complex interaction between silicate and carbonate matter, involving assimilation and carbonate–silicate unmixing. It was associated with basification, abundant crystallization of spinel and fassaite, and oversaturation of the silicate system with Ca. This model is substantiated by the spatial confinement of the Ambinsky volcanic edifice to the outcrops of marbled limestones and the heavy oxygen isotope composition. The maximum accumulation of Ca and CO_2 fluid in the silicate system makes it unstable and leads to immiscibility with exsolution of carbonate liquid. Microdrops of carbonate globules in silicate melts serve as evidence for the existence of two equilibrium unmixing liquids.

The thermal decomposition of carbonates with dissolution of CaO in the basaltic magma and accumulation of CO_2 in a closed magmatic chamber repeatedly produced the autoclave gas effect, which caused explosive eruptions atypical of this type of basalts.

The genesis of the carbonatite tuffs of the Ambinsky volcano is a model example of exsolution of carbonate melt in a moderately alkali nonagpaitic basaltic system.

REFERENCES

1. B. I. Vasil'ev, *Explanatory Note to Map Scale 1 : 200 000. Sheet K-52-XII, XVIII* (Gosgeoltekhizdat, 1961) [in Russian].

2. A. V. Girnis, V. K. Bulatov, and G. P. Brey, "Transition from Kimberlite to Carbonatite Melt under Mantle Parameters: An Experimental Study," Petrologiya **13**, 9–18 (2005) [Petrology **13**, 1–15 (2005)].

3. E. P. Denisov, "Composition of Augite Inclusions in Alkaline Basaltoids," Geol. Geofiz. **14** (3), 34–41 (1973).

4. M. I. Dubrovskii, "Origin of Carbonate–Aluminosilicate Magmas," Zap. Vseross. Miner. O-va, No. 6, 8–29 (2004).

5. S. V. Esin, V. M. Logvinov, and I. A. Ashchepkov, "Megacrystals of Aluminous Clinopyroxenes from Alkaline Basaltoids in the Minusa Depression of the Baikal Rift Zone and the Eastern Sikhote Alin," Geol. Geofiz. **34** (7), 101–110 (1993).

6. A. F. Efimov, *Typomorphism of Rock Forming Dark-Color Minerals of Alkaline Rocks* (Nauka, Moscow, 1983) [in Russian].

7. Yu. D. Zakharov, N. G. Boriskina, and A. M. Popov, *Reconstruction of Late Paleozoic and Mesozoic Conditions of Marine Environment From Isotopic Data with Reference to North Eurasia* (Dal'nauka, Vladivostok, 2001) [in Russian].

8. V. V. Ivanov, L. G. Kolesova, A. I. Khancuk, et al., "Find of Diamond Crystals in Jurassic Rocks of the Meymechite–Picrite Complex in the Sikhote Alin Orogenic Belt," Dokl. Akad. Nauk **406**, 72–75 (2005) [Dokl. Earth Sci. **404** 975–978 (2005)].

9. V. A. Kononova, *Urtite–Ijolite Intrusions in Southeastern Tuva and Their Origin* (Izd. Akad. Nauk SSSR, Moscow, 1961) [in Russian].

10. S. O. Maksimov, V. G. Moiseenko, and V. G. Sakhno, "High-K Basalts of Eruptive Pipes from the Eastern Part of the Bureya Massif, Russian Far East" Dokl. Akad. Nauk **379** (6), 797–801 (2001) [Dokl. Earth Sci. **379A** (6), 640–643 (2001)].

11. S. O. Maksimov and V. K. Popov, "Carbonate–Silicate Immiscibility in Basaltoids and the Origin of Crustal Carbonatites," in *Proceedings of Annual Seminar on Geochemistry of Magmatic Rocks. Works of Scientific School of Alkaline Magmatism of the Earth* (GEOKHI, Moscow, 2005), pp. 102–105 [in Russian].

12. S. O. Maksimov and V. K. Popov, "The First Finding of Carbonatite Tuffs in Cenozoic Basaltic Volcano of Southeastern Primorye," Dokl. Akad. Nauk **408**, 375–380 (2006) [Dokl. Earth Sci. **408**, 617–622 (2006)].

13. A. A. Marakushev and N. I. Suk, "Carbonate–Silicate Magmatic Immiscibility and Carbonate Genesis," Dokl. Akad. Nauk **360** (5), 681–684 (1998) [Dokl. Earth Sci. **361** (5), 696–699 (1998)].

14. *Minerals. Reference Book*, ed. by N. N. Smol'yaninov (Nauka, Moscow, 1981), Vol. III, No. 2 [in Russian].

15. L. L. Perchuk, *Thermodynamic Regime of Deep Petrogenesis* (Nauka, Moacow, 1973) [in Russian].

16. B. G. Pokrovskii, *Crustal Contamination of Mantle Magmas from Isotopic Geochemistry Data* (Nauka, Moscow, 2000) [in Russian].

17. V. K. Popov, S. V. Rasskazov, I. Yu. Chekryzhov, et al., "K–Ar Dating and Geochemistry of Cenozoic Trachybasalts and Trachyandesites in Primorye," in *Proceedings of Annual Seminar on Geochemistry of Magmatic Rocks. Works of Scientific School of Alkaline Magmatism of the Earth* (Geochim. Inst. Ross. Akad. Nauk, Moscow, 2005), pp. 133–135 [in Russian].

18. S. V. Rasskazov, E. V. Yasnygina, E. V. Saranina, et al., "Cenozoic Magmatism in Southwestern Primorye: Pulse Melting of the Mantle and Crust," Tikhookean. Geol. **23** (6), 3–31 (2004).

19. *Decisions of the 4th Stratigraphic Conference on the Precambrian and Phanerozoic in the Southern Far East and the Eastern Transbaikal Region, Khabarovsk, 1990* Preprint (Khabarovsk. KHGGGP, Khabarovsk, 1994) [in Russian].

20. V.S. Samoilov, *Carbonatites: Facies and Formation Conditions* (Nauka, Moscow, 1977) [in Russian].

21. A. A Syas'ko, A. A. Vrzhosek, A. P. Dubinskii, et al., *State Geological Map of RF. Scale 1 : 200 000. Sikhote Alin Series. Sheet K-52-XII, XVIII. Explanatory Note* (St. Petersburg, 2002) [in Russian].

22. S. A. Shcheka, *Basite–Hypebasite Intrusions and Inclusions in Extrusive Rocks of Russia's Far East* (Nauka, Moacow, 1983) [in Russian].

23. A. R. Basu, W. Junwen, H. Wankang, et al., "Major Element, REE, and Pb, Nd, and Sr Isotopic Geochemistry of Cenozoic Volcanic Rocks of Eastern China: Implications for Their Origin from Suboceanic-Type Mantle Reservoir," Earth Planet.Sci. Lett. **105** (1–3), 149–169 (1991).

24. R.J. Bultitude and D. H. Green, "Experimental Studu of Crystal–Liquid Relationship at High Pressure in Olivine Nephelenite and Basanite Compositions," J. Petrol. **1** (12), 121–147 (1971).

25. J. B. Dawson, "Perkaline Nephelinite-Natrocarbonatite Relationship at Oldoinyo Lengai, Tanzania," J. Petrol. **39** (11–12), 2077–2094 (1998).

26. D. H. Eggler, "The Effect of CO_2 upon Partial Melting of Peridotite in the System Na_2–CaO–Al_2O_3–MgO–SiO_2–CO_2 to 35 kb, with an Analysis of Melting in a Peridotite H_2O–CO_2 System," Am. J. Sci. **278** (3), 305–343 (1978).

27. Q. Fan and P. R. Hooper, "The Cenozoic Basaltic Rocks of Eastern China: Petrology and Chemical Composition," J. Petrol. **32** (4), 765–810 (1991).

28. J. Ferguson and K. L. Currie, "Evidence of Liquid Immiscibility in Alcaline Ultrabasic Dikes at Callander Bay, Ontario," J. Petrol **12** (3), 561–585 (1971).

29. I. C. Freestone and D. L. Hamilton, "The Role of Liquid Immiscibility in the Genesis of Carbonatites an Experimental Study," Contrib. Mineral. Petrol. **73** (2), 105–117 (1980).

30. V. A. Kjarsgaard and D. L. Hamilton, "Liquiol Immiscibility and Origin of Alkali-Poor Carbonatites," Miner. Magazine **52** (1), 43–55 (1988).

31. R. W. Le Maitre, P. Bateman, A. Dudek, *et al.*, *A Classification of Igneous Rocks and Glossary of Terms*, Ed. by R. W. Le Maitre (Blackwell, Oxford, 1989).

32. M. Meschede, "A Method of Discriminating between Different Types of Mid-Ocean Ridge Basalt and Continental Tholeiites with the Nb–Zr–Y Diagram," Chem. Geol. **56** (3), 207–218 (1986).

33. J. A. Pearce and J. R. Cann, "Tectonic Setting of Basic Volcanic Rocks Determined Using Trace Element Analysis," Earth Planet. Sci. Lett. **19** (2), 290–300 (1973).

34. S. -S. Sun, "Chemical Composition and Origin of the Earth's Primitive Mantle," **46** (2), 179–192 (1982).

35. S. -S. Sun and W. F. McDonough, "Chemical and Isotopic Systematics of Oceanic Basalts: Implications for Mantle Composition and Processes," in *Magmatism in the Ocean Basins,* Ed. by A. D. Sounders and M. J. Norry (Geol. Soc. Spec.Publ.,1989), No. 42, pp. 313–345.

Recommended for publication by A.V. Koloskov.

DISCUSSION

Could Carbonatite Matter That Was Mobilized by Alkali Basaltic Melts from Exogenic Carbonates Be Ascribed to Carbonatites?

S. V. Rasskazov

Institute of the Earth's Crust, Siberian Division, Russian Academy of Sciences, Irkutsk, Russia

Popov with coauthors [6] claimed the discovery of Oligocene–Miocene carbonatites in Southwestern Primorye. The 6-Ma-old high-alkali melilite–olivine nephelinites, the derivatives of a carbonatized mantle source, are known from southwestern Japan [12]. Therefore, the find of young carbonatites in southwestern Primorye is of special importance for revealing the structural conditions of the evolution of this type of magmatism on the continental margin and for prospecting of young mineralization. Unfortunately, attempts of Popov and coauthors to consider these carbonate rocks as carbonatites dismiss other genetic models.

It was suggested in this paper that the pyroclastic volcanic rocks (tuffs and others) were formed owing to

volatile release from the melt. Hence, the rocks must have pores. In Miocene lavas, pores are typically filled with secondary carbonate–radial aragonite; tabular calcite; and, occasionally, amorphous dolomite. No explanation is given with respect to the composition of the matrix that hosts the oval carbonatite inclusion in Photo 2a. Ovoids that differ in composition from the matrix were described in the lavas of the southern Russian Far East in the works of S.A. Shcheka, A.A. Vrzhosek, V.K. Popov, and others. Oval inclusions could result from liquid immiscibility of silicate liquids or mixing of two melts, one of which could be volatile-rich, providing formation of pores and their filling with secondary carbonate. Thus, the ocellar carbonates could be unrelated with carbonatites.

Popov and others believe that the oval calcite inclusions are unmixing ocelli. It is known that liquid immiscibility is the splitting of a homogenous melt into two immiscible liquids. Since tuffs are welded clastic rocks, the mechanism of liquid immiscibility cannot be applied to the formation of carbonate ocelli. Therefore, carbonate inclusions in tuffs are either pores filled with secondary carbonate, crystals rounded during explosive mechanical erosion (fragments of carbonate rocks), or entrained terrigenous material rounded in water streams.

The terminological questions in geology are still debatable. Petrographic terminology is underlain by the rock genesis. According to definition [2], carbonatites are carbonate rocks of intrusive or effusive origin that either associate with basic or ultrabasic alkali rocks or occur independently. They typically bear rare-metal mineralization and contain pyrochlore, apatite, phlogopite, and others as typomorphic minerals [3]. Carbonates are common minerals of alkaline magmatic complexes, where they either are scattered over silicate rock (kimberlites, alkali granites) or form independent bodies. There are eight types of rare metal carbonatites [1, 10]. Their origin is typically related to carbonate-rich mantle or crustal magmatic sources. Some mantle sources of basaltic melts contain carbonate, but their evolution does not always lead to carbonatite production. The high contents of rare-earth and other trace elements in carbonatites reflect equilibrium evolution of deep-seated magmatic melts, which is controlled by the trace element partition coefficient between mineral phases, fluids, and residual melts, and sometimes involve liquid immiscibility of silicate and carbonate liquids. Geochemical study showed that alkali ultramafic complexes were formed by mixing of two and more sources, with carbonatites as the final mixing product [9].

Could the carbonates have crystallized from basanite melts of Ambinsky volcano? Fluids of these melts are enriched in CO_2 [4]. The study of Cenozoic volcanic fields in Central Asia showed that volatiles are exsolved from high alkali basanite melts in magmatic channels. The eruption of volatile-rich melts results in the formation of pyroclastic cones, while ejected basanite lavas often lack volatiles and have no pores in the flow bottom and roof. With increasing water content in the moderately alkaline lavas (alkali basalts, hawaiites, olivine tholeiites), the volatiles are exsolved immediately in the flow, thus producing the bottom layer of cable basalts and the thick pore-rich top layer [7]. Thus, the high content of CO_2, in combination with excess Ca in high-alkali basanites, could produce high carbonate activity.

Considering the carbonate sources, Popov and coauthors made contradictory statements in their comments. On the one hand, they suggest that the leading mechanism in the formation of the Ambinsky carbonatites was the assimilation of marbled limestones of the Barabash Formation by basanite melts and, on the other hand, arrive at the opposite conclusion of the mantle origin of the carbonatite source based on the carbon and oxygen isotope composition. It should be noted that the proportions of light and heavy carbon and oxygen isotopes do not reflect the source composition but result from crystallization differentiation [5]. The carbon and oxygen isotope composition of the carbonates from two samples of Ambinsky volcano attests to their high-temperature formation.

Controversial interpretations have been proposed in the literature to explain the origin of carbonate rocks that differ from typical rare-metal carbonatites in the absence of typomorphic minerals and a low content of rare metals (Table). These carbonate (or carbonate-bearing) bodies could have sharp contacts and represent either skarns or high-temperature hydrothermal veins. In addition, exogenic carbonates could be entrained as xenoliths (such as granites, gneisses, and other rocks) and crystallize as individual crystals or aggregates. There is also the hypothesis that carbonatites result from melting in different geodynamic settings and that magmatic hydrothermal skarns and some carbonate systems cannot be distinctly distinguished [11, 13, and references in these works].

The controversial interpretation can be exemplified by the Ulsan carbonates of the Cenozoic Gyeongsang depression in southeastern Korea. They form a vertical body 150–200 m across in serpentinites, contain a large magnetite pipe with scheelite and arsenopyrite, and are cut by the Early Tertiary basic dikes. Two types of carbonates are distinguished there: (1) white milk fine-grained calcite and (2) purely white coarse-grained (up to 5 cm) calcite associated with basic dikes, magnetite ore, and metasomatic mineralization. Calcite I has $\delta^{13}C_{PDB}$ from 2.4 to 4.0 and $\delta^{18}O_{SMOW}$ from 9.8 to 11.2, which are close to the isotope composition of marine limestones, while these values in calcite II are, respectively, 10.3–11.1 and 9.8–11.2, which is typical of magmatic calcites [13].

Creamy carbonates that compose a 0.5 m thick vein in the Ekhe–Shigna River basin, the left tributary of the Urik River, East Sayan, do not contain typomorphic accessory minerals of carbonatites. Analytical studies

Contents of major (wt %) and trace (ppm) elements in the carbonate and carbonate-bearing rocks

Ordinal Number	1	2	3	4	5
Sample No.	5539/2	UC1	UC8	C-2001/18	23-b
SiO_2	30.93				0.08
TiO_2	1.13				0.02
Al_2O_3	12.62				Not determined
Fe_2O_3	3.04				Not determined
FeO	2.34				0.50
MnO	0.46				0.31
MgO	4.60				0.15
CaO	22.72		Not determined		56.04
Na_2O	0.90				0.12
K_2O	0.56				Not determined
P_2O_5	0.23				Not determined
H_2O^-	1.79				Not determined
	4.91				Not determined
CO_2	13.95				42.35
Cy	100.18				99.63
Sc	Not determined		Not determined	0.85	4.12
Rb	23			0.95	9.1
Sr	518	245	72	1630	16622
Y	18	2	4	13	254
Zr	90	2	2	3.2	Not determined
Nb	13	1	1	0.74	1.65
Cs	5.31	Not determined		0.08	Not determined
Ba	527	Not determined		134	933
La	19	0.76	0.85	30	977
Ce	30	0.59	1.59	34	1749
Pr	39(?)	0.18	0.34	3.9	213
Nd	18	0.50	1.29	17.3	723
Sm	3.3	0.11	0.33	3.05	75.7
Eu	1.13	0.02	0.13	0.56	18.5
Gd	3.7	0.16	0.34	1.95	52.3
Tb	0.56	0.02	0.07	0.26	8.83
Dy	3.23	0.14	0.41	2.24	30.3
Ho	0.6	0.03	0.08	0.45	5.46
Er	2.12	0.12	0.27	0.97	17.1
Tm	0.26	0.02	0.04	0.2	Not determined
Yb	1.42	0.11	0.23	1.15	11.0
Lu	0.21	0.02	0.03	0.19	1.62
Hf	2.7			0.14	Not determined
Ta	5.31	Not determined		0.09	0.13
W	Not determined			0.22	Not determined
Pb	4.5	3	3	17.8	10.1
Th	2.18	1	1	1.75	1.46
U	0.69	1	1	1.09	0.07
Sr/Pr	?	1360	212	417	78
Ce/Pb	6.7	0.2	0.53	1.9	173
La/Yb	13	6.9	3.4	26	89

Note: (1) "carbonatite" tuff of Ambinsky volcano [6]; (2–3) Ulsan carbonates, respectively, of types I and II [13]; (4) hydrothermal carbonate vein of the Ekhe Shigna River (unpublished results of ICP-MS study at the Laboratory of Isotope and Geochronology of the Earth's Crust Institute; sample was given by V.P. Sekerin and Yu.V. Men'shagin, prepared for analysis by M.E. Markova, and analyzed using a Plasma Quad 2+ mass spectrometer); (5) carbonatite vein of the Zadoi (Zhidoi) alkali–ultramafic massif (Eastern Sayan) [9].

showed that they have high contents of Sr (1630 µg/g) at a low REE content (Table) and high $^{87}Sr/^{86}Sr$ ratio (0.709356), which is comparable with that in the Lower Paleozoic carbonates of this area. The vein presumably is of high-temperature hydrothermal origin.

As compared to the rare-metal carbonatites, carbonate rocks of exogenous origin that were redeposited during magmatism or high-temperature hydrothermal process are depleted in rare metals at a high Sr/Pr ratio and low La/Yb and Ce/Pb ratios (table).

Could the carbonates redistributed from exogenous carbonates into an alkali basaltic melt be considered as carbonatite? Carbonate segregations often occur in the outer contacts of basanite magmatic channels. Euhedral crystals of creamy carbonate up to 2 cm in size were found, for instance, in the outer contact zone of the Miocene basanite neck at the Kamar Range on the southwestern coast of Lake Baikal [8]. Carbonate was entrained from the host rocks of the Slyudyanka Group. The high-temperature basanite melt presumably caused mobilization and assimilation of carbonate. The geochemistry of these crystals was not studied, but their geological position unambiguously indicates the xenogenic origin of the carbonate matter.

Popov and colleagues established the interesting geological fact that high-temperature alkali basaltic melts assimilate exogenous carbonates in shallow conditions. However, interpretation of this fact as the occurrence of carbonatite magmatism is ambiguous. Carbonate material that crystallized, together with silicates, was not produced by equilibrium evolution of a mantle basanite melt but is of foreign origin. The origin of the rocks under discussion was related to mixing of two sources in the upper crust: a deep-seated mantle source that produced a basanite melt and a shallow crustal source of exogenic carbonates. Such an interaction between magmatic material and carbonates can be termed as skarn formation. This process differs from formation of rare-metal carbonatites through mixing of deep-seated mantle melts; hence, these rocks should be referred to as carbonatite-like rocks

REFERENCES

1. Yu. A. Bagdasarov, "On the Main Petrochemical and Geochemical Peculiarities of Linear Carbonatites and Their Formation Conditions," Geokhimiya **28** (8), 1108–1119 (1990).

2. *Glossary of Geology* (Moscow, 1978), Vol. 1 [in Russian].

3. Yu. L. Kapustin, *Minerals of Carbonatites* (Nauka, Moscow, 1971) [in Russian].

4. B. O. Mysen and A. L. Boettcher Melting of a hydrous mantle (J. Petrol. **16**, 530–293; Mir, Moscow, 1979) [in Russian].

5. G. S. Plyusnin, V. S. Samoilov, and S. I. Golyshev, "Method of Isotopic Pairs of ^{13}C, ^{18}O and the Temperature Facies of Carbonatites," Dokl. Akad. Nauk SSSR **254** (5), 1241–1245 (1980).

6. V. K. Popov, S. O. Maksimov, A. A. Vrzhosek, and V. M. Chubarov, "Basaltic and Carbonatite Tuffs of Ambinsky Volcano (Southwestern Primorye): Geology and Origin," Tikhookean. Geol. **26** (4), 75–93 (2007).

7. S. V. Rasskazov, *Fluid Regime of Cenozoic Volcanism in South Siberia* Available from Vses. Inst. Ekon. Mineral. Syr'ya, No. 385-MG (Moscow, 1987) [in Russian].

8. S. V. Rasskazov, *Magmatism of the Baikal Rift System* (Vost. Otd. Nauka. Sib. Izd. Firma, Novosibirsk, 1993) [in Russian].

9. S. V. Rasskazov, A. A. Konev, A. M. Il'yasova, et al., "Zadoisky (548 M.Y.) Geochemical Evolution of the Zadoi Alkaline-Ultramafic Massif, Cis-Sayan Area, Southern Siberia," Geokhimiya **44** (1), 3–18 (2007) [Geochem. Int. **44** (1), 1–14 (2007)].

10. N. A. Solodov, "Genetic Types of Rare Metal Carbonatites," Otech. Geol., No. 9, 12–18 (1996).

11. D. Lentz, "Carbonatite Genesis: A Reexamination of the Role of Intrusion-Related Pneumatolytic Skarn Processes in Limestone Melting," Geology **27**, 335–338 (1999).

12. Y. Tatsumi, R. Arai, and K. Ishizaka, "The Petrology of a Melilite-Olivine Nephelinite from Hamads, SW Japan," J. Petrol. **40** (4), 497–509 (1999).

13. K. Yang, J-Y. Hwang, and S-H. Yun, "Petrogenesis of the Ulsan Carbonate Rocks from the South-Eastern Kyongsang Basin, South Korea," The Island Arc **12**, 411–422 (2003).